

Novel Red Emitting Iridium(III) Complexes Based on Methoxy Substituted Phenylquinoline for Organic Light-Emitting Diodes

H.K. Dahule¹, S.J.Dhoble², Neha Khotale³, Minakshi Ghate⁴

^{1,3,4}Department of Physics Shivaji Science College, Congress Nagar, Nagpur-440012, India

²Department of Physics, Rashtrasant Tukadoji Maharaj Nagpur University, Nagpur 440033, India

Abstract: A new series of highly efficient Ir(III) complexes, $(OMe-DPQ)_2Ir(acac)$, $(Cl-OMe-DPQ)_2Ir(acac)$, were synthesized for phosphorescent organic light-emitting diodes (PhOLEDs), and their photophysical, electrochemical, and electroluminescent (EL) properties were investigated. The Ir(III) complexes, including acetyl acetone (acac) as ancillary ligand, are comprised with the various main ligands such as 2-(4-Methoxy-phenyl)-4-phenyl-quinoline(OMe-DPQ), 4-chloro-2-(4-Methoxy-phenyl)-4-phenyl-quinoline (Cl-OMe-DPQ). The synthesized iridium metal complexes, $(OMe-DPQ)_2Ir(acac)$, $(Cl-OMe-DPQ)_2Ir(acac)$, is characterized by employing various techniques such as mass spectrometry, ¹HNMR, DTA/TGA, XRD, and FTIR. The molecular structures of complexes are confirmed by the FTIR spectra. A strong ¹MLCT (singlet metal-to-ligand charge-transfer) and ³MLCT (triplet metal-to-ligand charge-transfer) absorption peaks at 270,330,354,427,465,510 nm in tetrahydrofuran (THF) solution are reported in $(OMe-DPQ)_2Ir(acac)$ complex. $(Cl-OMe-DPQ)_2Ir(acac)$ shows strong ¹MLCT and ³MLCT absorption peak at 263, 335, 442, 479, 508 and 539 nm in dichloromethane solution. The OMe-DPQ exhibits the photoluminescence (PL) peaks at 434 nm when excited at 385 nm. in powder, at 407 and 430 nm when excited at 367 in chloroform and THF solution respectively. A red emitting PL peak at 610 nm with the Commission International de l'Eclairage (CIE) coordinates of (0.662, 0.333) is observed in $(OMe-DPQ)_2Ir(acac)$ complex. The Cl-OMe-DPQ exhibits the photoluminescence (PL) peaks at 439 nm when excited at 385 nm. in powder, at 409 and 436 nm when excited at 367 in chloroform and THF solution respectively. A red emitting PL peak at 619 nm with the Commission International de l'Eclairage (CIE) coordinates of (0.683, 0.312) is observed in synthesized $(Cl-OMe-DPQ)_2Ir(acac)$ complex. The soluble red emitting $(OMe-DPQ)_2Ir(acac)$ $(Cl-OMe-DPQ)_2Ir(acac)$ complexes in common organic solvents is promising for flexible organic devices.

Keyword: Synthesis, (OMe-DPQ),(Cl-OMe-DPQ),Iridium complexes, photoluminescence

1. Introduction

Organic light-emitting diodes (OLEDs) are being most extensively researched for many applications, including flat-panel displays and solid-state lightings [1,2]. Internal quantum efficiencies near unity, corresponding to the harvesting of all singlet and triplet states, can be achieved in OLEDs composed of phosphorescent complexes based on ligated iridium (Ir), platinum, ruthenium, and osmium. As of now available light-emitting materials, phosphorescent iridium (Ir) complexes are particularly promising because they can emit the light from both singlet and triplet excitons, enabling the fabrication of phosphorescent organic light-emitting diodes (PhOLEDs) with close to 100% internal quantum efficiency [3,4]. The efficiencies, brightness, and wavelength emissions of Ir(III) complexes strongly depend on the molecular structure of a cyclometalated ligand. The emission wavelength of Ir(III) complexes normally can be altered by changing the electron density or position of substituents on the main ligands. For example, emission wavelengths of these Ir(III) complexes can be adjusted to cover the entire visible spectral region by modifying or varying cyclometalated 2,4-diphenyl quinoline (DPQ) ligands [5–8]. Therefore, the design and preparation of novel cyclometalated ligands for Ir(III) complexes has attracted great attention. The most well-known fabrication strategies for the PhOLEDs are thermal evaporation and solution processing methods. The thermal deposition enables the formation of complicated multilayer device architectures for excellent device perform with high efficiencies [9,10].

However, it is not easy to form the multistacked layers of organic materials by the solution processing method since the solvent used for depositing organic materials usually causes unwanted swelling and/or damage to the previously coated layers [11]. For this reason, the performance of PhOLEDs based on the thermally evaporated thin films is generally better than that of the solution processed PhOLEDs. Apart from the above-mentioned limitation, however, the solution processing has several advantages, including its simplicity, manufacture ability on a large scaled area, extremely low-cost, and can be extended to large area substrates, and to high-throughput reel-to-reel processing [12–14]. Additionally, it is possible to realize co-doping of several dopants by mixing the dopants and host material in solution. Thus, many research groups are still focused on the synthesis of suitable materials for the solution fabrication processes to improve the device performance [15].

The iridium complexes used in electroluminescent (EL) devices are octahedral with a 3+ oxidation state and the observed luminescence is the emission from a triplet MLCT (metal-to-ligand charge-transfer) state or a ligand-based ³(π - π^*) excited state. The organic ligands in the complexes are generally a heterocycle that coordinates to the metal center via the formation of an Ir-N and Ir-C bond. Both the EL efficiency and the emission wavelength of Ir complex based devices are affected greatly by this organic ligand.[16] The synthesis of efficient red emitters is intrinsically more difficult because their luminescence quantum yields tend to decrease as the emission wavelength increases in accordance

with the energy gap law.[18] The emission colors from these complexes, which range from blue to red, are strongly dependent on the choice of the cyclometalating ligand.[16, 17- 28] Thus, the design and synthesis of new organic ligands for Ir complexes is highly desirable.

In this paper, we have demonstrated red light emitting iridium complexes and studied optical properties in various solvents. We have synthesized a 2-(4-Methoxy-phenyl)-4-phenyl-quinoline(OMe – DPQ) and 4-chloro-2-(4-Methoxy-phenyl)-4-phenyl-quinoline (Cl-OMeDPQ). ligand and it is used as a ligand to synthesize the red iridium complexes [(OMe-DPQ)₂ Ir (acac)], [(Cl-OMe-DPQ)₂Ir(acac)], instead of common isoquinoline ligand. The absorption and emission of the ligand and the complex in the visible region was measured in different organic solvents such as acetic acid, formic acid, Chloroform, dichloromethane, and tetrahydrofuran (THF). The red light emission at 610 nm and 619 nm is reported in this complexes.

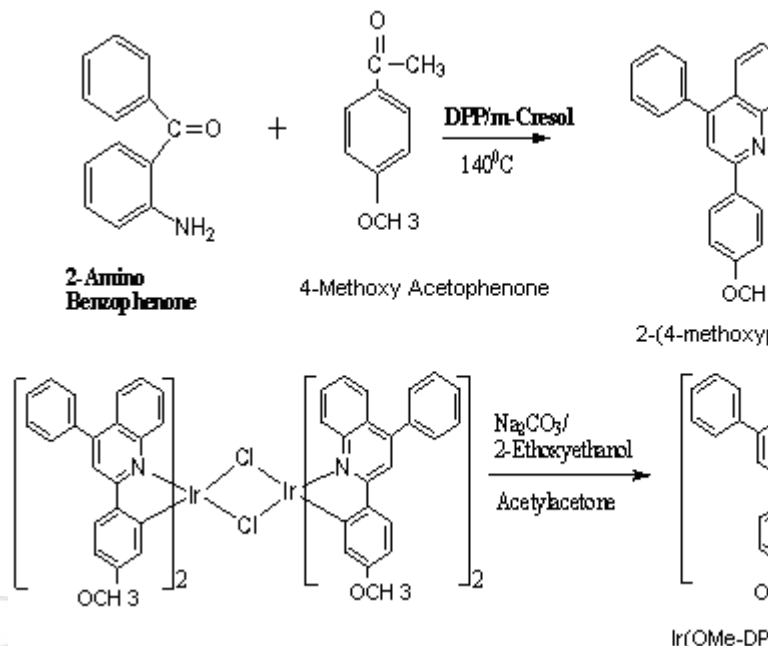
2. Experimental

2.1 Synthesis of 2-(4-Methoxy-phenyl)-4-phenyl-quinoline (OMe –DPQ):

The quinoline-derived ligand 2-(4- Methoxy-phenyl)-4-Phenyl quinoline (OMe-DPQ), were synthesized conveniently according to Scheme 1 from the condensation of 2-Aminobenzophenone and 4-methoxy acetophenone using the acid-catalyzed Friedlander reaction [23]. 2-Aminobenzophenone (2gm), and 4-methoxy acetophenone (2gm), were added along with Di-phenyl Phosphate (DPP) (2 gm), and m-Cresol (3 ml), in a glass reactor fitted with mechanical stirrer, two glass inlets and one side arm.

The reaction mixture was purged with argon for 20 min. and then the temperature was raised to 90 °C gradually under Argon atmosphere (99% pure) for 1 hour and subsequently to 140 °C for 4 hours. After cooling, dichloromethane-CH₂Cl₂, (50 ml) and 10 % NaOH (50 ml) were added to the reaction mixture.

The organic layer was separated and washed with distilled water (20 ml x 5) until it was neutral, then dried over MgSO₄ and evaporated under vacuum to yield an off- white solid with some radish liquid on top. The crude product was filtered and washed with hexane (5 ml x 3) to obtain crystalline solid of 2-(4-Methoxyphenyl)-4-Phenylquinoline abbreviated as (OMe-DPQ),.



Scheme1: Synthesis of [2- 4- methoxy phenyl, 4-phenyl quinoline] (OMe-DPQ) and [(OMe-DPQ)₂ Ir (acac)] Complex

The crude product then washed with hexane (25 ml x 5 times) to afford crystalline solid [C₂₂H₁₇NO] , mol. wt. = 311.242 gm.

Yield: 73%. ¹H NMR (300 MHz, CDCl₃): δ 3.90 (s, 3H), 7.06 (d, J = 8.6 Hz, 2H), 7.46 (td, J = 7.6, 1.2 Hz, 1H), 7.53–7.58 (m, 5H), 7.72 (td, J = 7.6, 1.2 Hz, 1H), 7.79 (s, 1H), 7.89 (d, J = 8.4 Hz, 1H), 8.19 (d, J = 8.6 Hz, 2H), 8.24 (d, J = 8.5 Hz, 1H).

2.2 Synthesis of Bis (2-(4-methoxy-phenyl)-4-phenyl quinoline)iridium(acetylacetonate) [(OMe-DPQ)₂ Ir (acac)] Complex (OMe-DPQ)₂ Ir (acac) was synthesized according to scheme 1. (OMe-DPQ) (.770g, 2.2mmol) was dissolved in ethoxy ethanol(10ml) in a 50ml round bottom flask . Iridium trichloride hydrate [IrCl₃.3H₂O](.2984 gm ,1 mmol) and 3ml of water were then added to the flask. The mixture was stirred under argon at 120 °C for 24hr.The mixture was cooled to room temperature and the precipitate was collected and then dried to give a cyclometallated chloride bridged dimer as red powder. In a 50 ml flask, the chloride bridged dimer, acetyl acetone (1.0 m mol)and Na₂CO₃ (2.5 m mol) were dissolved in 2ethoxyetenol(15 ml) and the mixture was the refluxed under a argon atmosphere for 12 h. After cooling to room temperature, the precipitate was filtered off and washed with water ,ethanol and ether give to desire pure complex.

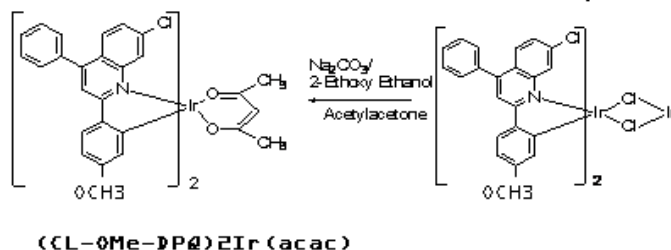
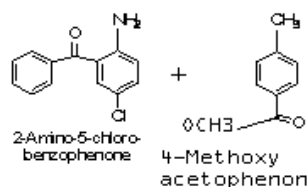
Yield: 48%. Anal. Calcd for C₄₉H₃₉N₂O₄Ir: C, 64.53; H, 4.31; N, 3.07.Found: C, 64.18; H, 4.26; N, 2.99.

¹HNMR(300 MHz, CDCl₃):δ 1.56 (s, 6H), 3.43 (s, 6H), 4.73 (s, 1H), 6.13 (d, J = 2.4 Hz,2H), 6.52 (dd, J = 8.6, 2.2 Hz, 2H), 7.36 (t, J = 7.4 Hz, 2H), 7.43(t, J = 7.5 Hz, 2H), 7.55–7.68 (m, 10H), 7.75 (d, J = 8.6 Hz, 2H),7.80 (d, J = 8.0 Hz, 2H), 7.88 (s, 2H), 8.57 (d, J = 8.6 Hz, 2H).

2.3 Synthesis of 4-chloro-2-(4-Methoxy-phenyl)-4-phenyl-quinoline (Cl-OMe-DPQ).

The quinoline-derived ligand 4-Chloro-2-(4-Methoxyphenyl)-4-Phenylquinoline (Cl-OMe-DPQ), were synthesized conveniently according to Scheme 2 from the condensation of 2-Amino, 5-Chlorobenzophenone and 4-methoxy acetophenone using the acid-catalyzed Friedlander reaction [23]. 2-Amino, 5-Chlorobenzophenone (2gm), and 4-methoxy acetophenone (2gm), were added along with Diphenyl Phosphate (DPP) (2 gm), and m-Cresol (3 ml), in a glass reactor fitted with mechanical stirrer, two glass inlets and one side arm.

The reaction mixture was purged with argon for 20 min. and then the temperature was raised to 90 °C gradually under Argon atmosphere (99% pure) for 1 hour and subsequently to 140 °C for 4 hours. After cooling, dichloromethane-CH₂Cl₂, (50 ml) and 10 % NaOH (50 ml) were added to the reaction mixture. The organic layer was separated and washed with distilled water (20 ml x 5) until it was neutral, then dried over MgSO₄ and evaporated under vacuum to yield an off-white solid with some radish liquid on top. The crude product was filtered and washed with hexane (5 ml x 3) to obtain crystalline solid of 4-Chloro-2-(4-Methoxyphenyl)-4-Phenylquinoline, abbreviated as Cl-OMe-DPQ.



Scheme1: Synthesis of [6-chloro-2-(4-methoxy phenyl, 4-phenyl quinoline) (Cl-OMe-DPQ) and [(Cl-OMe-DPQ)₂Ir(acac)] Complex

2.4 Synthesis of (Cl-OMe-DPQ)₂ Ir (acac) complex

[(Cl-OMeDPQ)₂ Ir (acac)] were synthesized according to Scheme 2. Cl-OMe-DPQ (2.2mmol) was dissolved in 2-methoxyethanol (10ml) in a 50ml round bottom flask.

Iridium trichloride hydrate [IrCl₃.3H₂O] (1 m mol) and 3ml of water were then added into the flask. The mixture was stirred under argon atmosphere at 120 °C for 24 hrs. The mixture was cooled to room temperature and the precipitate was collected and then dried to give a cyclometallated chloride bridged dimer as red powder. In a 50 ml flask, the cyclometallated chloride bridged dimer, acetyl acetone (1.0 m mol) and Na₂CO₃ (2.5 m mol) were dissolved in 2ethoxyetenol (15 ml) and the mixture was the refluxed under an argon atmosphere for 12 hrs. After cooling to room temperature, the precipitate was filtered off and washed with water, ethanol and ether to give the desired product (Cl-

OMeDPQ)₂ Ir (acac) Yield 75.04 %. Anal. Calcd for C₄₉H₃₉N₂O₄IrCl: C, 64.25; H, 4.34; N, 3.08. Found: C, 64.20; H, 4.28; N, 3.01.

3. Results and Discussion

3.1. Synthesis and structural characterizations

Friedlander reaction [23] was used to synthesize quinoline ligands as shown in Scheme 1. and 2. Condensation of the ketone with the o-aminobenzophenone catalyzed by the acid gave corresponding quinolines in the yield of 64–75%. The synthesis of the bis cyclometalated iridium complexes of quinoline ligands involved two steps according to the literature [18]. IrCl₃.nH₂O was first reacted with an excess of quinoline ligand to form a Chloride-bridged dimer. Then the dimer can be easily converted to the desired product by replacing the bridging chloride with acetyl acetone ligand (acac). Complex was purified by column chromatography. The structures and purity of the complex were characterized by ¹H NMR and elemental analysis. The mononuclear complex is thermally stable up to 300–385 °C revealed by thermal gravimetric analysis (TGA). X-ray crystallographic studies have been carried out for [(OMe-DPQ)₂ Ir (acac)] and [(Cl-OMe-DPQ)₂ Ir (acac)]

3.2 Structural Properties

3.2.1 FTIR Spectra

Fourier Transform Infrared Spectroscopy (FT-IR) is an analytical technique used to identify organic materials. The molecular structures of polymeric compound are confirmed by FT-IR spectra. This technique measures the absorption of various infrared light wavelengths by the material of interest. The FT-IR spectra of the new OMe-DPQ chlorophore are as shown in Fig.1

On the basis of FT-IR spectra, the conversion of the reaction forming OMe-DPQ can be estimated. The peak at 846 cm⁻¹, is characteristic of paradisubstitution of the benzene ring (15). The aromatic CH vibration stretch appears at 3100–3000 cm⁻¹. The absorption corresponding to 2820 cm⁻¹, indicates the presence of methoxy (OCH₃) group. There is aromatic CC stretch bands (for the carbon-carbon bonds in the aromatic ring) at about 1500 cm⁻¹. The strong FT-IR peaks at 1663 and 1656 cm⁻¹ owing to the carbonyl groups are almost completely disappeared in OMe-DPQ. A new strong bands between 1600 and 1400 cm⁻¹ due to the imines (C=N) group and characteristic of the quinoline ring were observed. This is usually an excellent confirmation of the completion of cyclization reaction forming quinoline rings. The characteristic peaks of FT-IR spectra of OMe-DPQ are [3060, 3023, 2963, 2897, 2820, 2601, 2396, 2036, 1934, 1798, 1663, 1656, 1515, 1460, 1447, 1404, 1358, 1307, 1256, 1244, 1234, 1112, 1074, 1000, 970, 957, 831, 775, 734, 679, 647, 633, 615, 588, 549, 522].

FTIR Spectra of (OMe-DPQ)₂ Ir (acac) is shown in Fig.2. The peaks at 3444 and 3020 cm⁻¹ are due to the C-H stretching frequency of aromatic (C-H) ring. The peaks at 3100–3000 cm⁻¹ are due to the CH vibration stretch. The absorption corresponding to 2820 cm⁻¹, indicates the presence of methoxy (OCH₃) group. The peaks

between $1615\text{--}1700\text{ cm}^{-1}$ due to the C-N stretching frequency are noticed. The peak at 1670 cm^{-1} due to C-C bond. The peak 1750 cm^{-1} due to C=O stretching frequency and at 1242 cm^{-1} due to the C-N stretching frequency are noticed. The peak at 1450 cm^{-1} aromatic C=C bond. The peak between $1220\text{--}1260\text{ cm}^{-1}$ are due to aromatic C-O bond. The peak at $1040\text{--}1060\text{ cm}^{-1}$ is related to the C-O stretching frequency, while between $790\text{--}870\text{ cm}^{-1}$ are due to the $>\text{C}=\text{CH}$ bending.

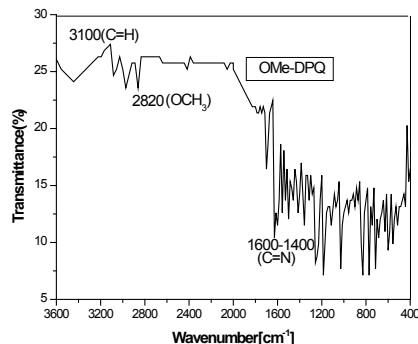


Figure 1: FT-IR spectra of OMe-DPQ

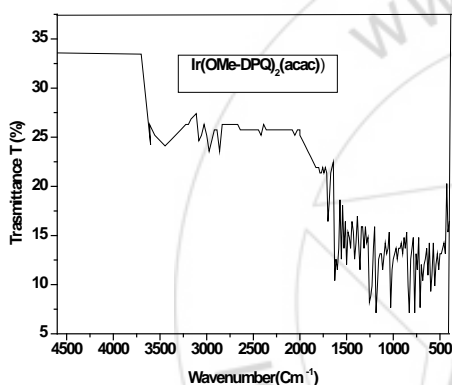


Figure 2: FT-IR spectra of $(\text{OMe-DPQ})_2 \text{Ir (acac)}$

FTIR Spectra of $(\text{CL-OMe-DPQ})_2 \text{Ir (acac)}$ is shown in Fig.3 The characteristic peaks of FT-IR spectra of $(\text{CL-OMe-DPQ})_2 \text{Ir (acac)}$ are at $3737, 3738, 3015, 2913, 2314, 1582, 1531, 1474, 1441, 1345, 1213, 1144, 1062, 1019, 966, 877, 830, 806, 768, 693\text{ cm}^{-1}$.

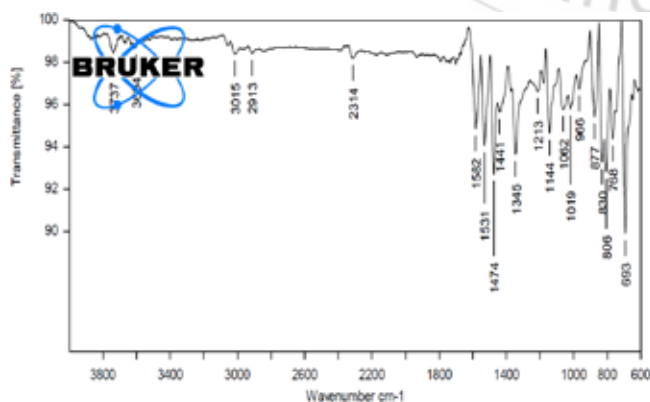


Figure 3: The FTIR spectra of $\text{Ir}(\text{CL-OMe-DPQ})_2(\text{acac})$

3.2.2 X-ray Powder Diffraction

The X-Ray diffraction pattern of Methoxy - Diphenyl Quinoline (OMe - DPQ) and $(\text{OMe-DPQ})_2 \text{Ir (acac)}$ and $(\text{CL-OMe-DPQ})_2 \text{Ir (acac)}$ are shown in Fig.4. and Fig 5. and Fig.6 respectively.

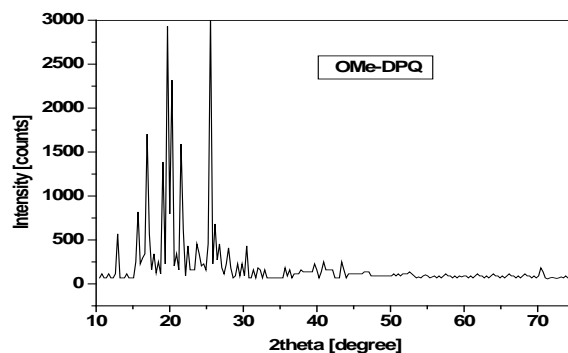


Figure 4: XRD pattern of OMe-DPQ

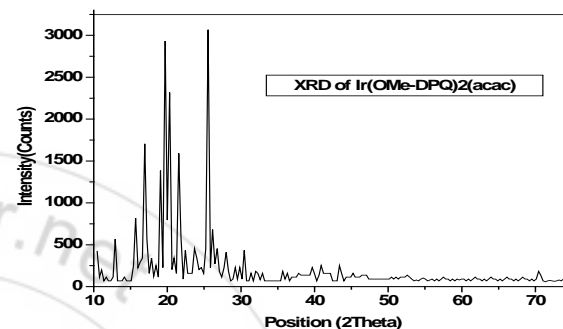


Figure 5: XRD pattern of $\text{Ir}(\text{OMe-DPQ})_2(\text{acac})$

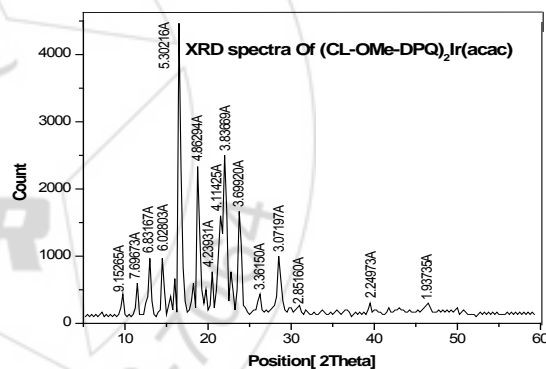


Figure 6: XRD pattern of $(\text{CL-OMe-DPQ})_2 \text{Ir (acac)}$

From the X-ray diffraction analysis, the powder OMe - DPQ $[(\text{OMe-DPQ})_2 \text{Ir (acac)}]$ and $[(\text{CL-OMe-DPQ})_2 \text{Ir (acac)}]$ have many strong, sharp diffraction peaks and some diffused background. This indicates the crystalline character of the compound. These spacings correspond to the chain distances of a well-organized molecular layer structure. A much weaker diffraction peak indicates lower crystallinity or orientation. In addition, its higher volume fraction of insulating side chains may also contribute to its low field-effect mobility. However, too much crystallinity causes brittleness. The crystallinity parts give sharp narrow diffraction peaks and the amorphous component gives a very broad peak (halo).

3.2.3 Thermal Properties

3.2.3.1 Thermo gravimetric Analysis (TGA) of $(\text{OMe-DPQ})_2 \text{Ir (acac)}$

The thermal stability of the complex $\text{Ir}(\text{OMe-DPQ})_2(\text{acac})$ was carried out from Thermo Gravimetric Analysis (TGA) and Single Differential Thermal Analysis (SDTA)

characterization in air atmosphere at heating rate 4 °C/min using Mettler STARE Thermo Gravimetric Analyzer, TGA/SDTA851e, coupled to a Balzers Thermo Star Mass Spectrometer. The TGA characteristics recorded are as shown in Fig. 7. From the Fig.7 it is clear that , no weight loss was observed in the first step of temperature range from 38 °C to 135 °C. i.e. there is no effect of temperature on a sample weight up to 135 °C .A small weight loss of about 0.794 % was observed in the second step of temperature range from 135 °C to 210 °C. The weight of the sample reduces to 12.4300 mg.

The weight loss of about 1.59 % was observed in the third step of temperature range from 210 °C to 240 °C. In this step, the sample weight becomes 12.331 mg.

3.2.3.2 Thermo gravimetric Analysis (TGA) of [(CL-OMe-DPQ)₂Ir(acac)]

The thermal properties of the complex were evaluated by means of TGA and DSC. Fig. 8 shows the TGA analysis of the [(CL-OMe-DPQ)₂Ir(acac)] when it was heated to 500 °C at a heating rate of 4 °C/min under a dry nitrogen atmosphere. The weight loss of the complex was less than 20 % upon heating to 300 °C, indicative of good thermal stability. The onset of thermal degradation is also shown in Fig. 8.

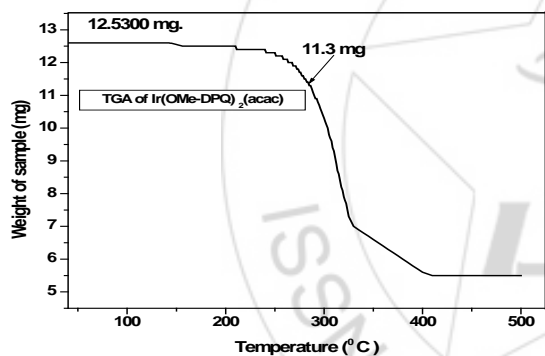


Figure 7: Thermogravimetric analysis of [Ir(OMe-DPQ)₂Ir(acac)]

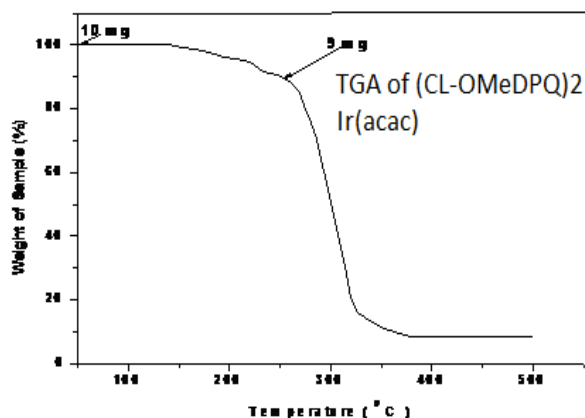


Figure 8: Thermogravimetric analysis of Ir(CL-OMe-DPQ)₂(acac)

3.2.3.3 Differential Scanning Calorimetry (DSC)

We investigated the thermal properties of [(OMe-DPQ)₂Ir(acac)] and OMe-DPQ by differential scanning calorimetry

(DSC) DSC measurement are recorded on Mettler Toledo System. The DSC second heating scans of the polymeric compound are as shown in Figure 9 Fig.9 indicate that OMe-DPQ undergoes a glass transition at 42°C, following by crystallization at 95°C and crystalline melting point at 425 °C. In contrast, there was no phase transition signal observed for Ir(OMe-DPQ)₂(acac) from 30 to 350 °C.

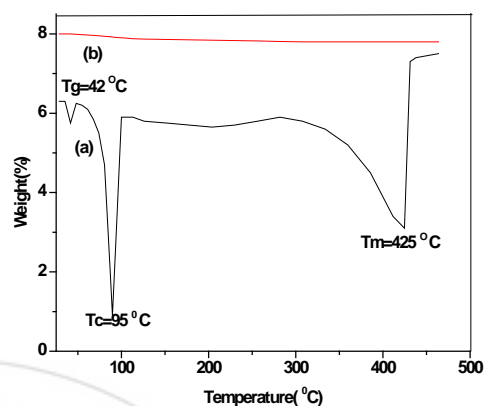


Figure 10: DSC scans of (a) OMe – DPQ and (b) [(OMe-DPQ)₂ Ir(acac)]

The DSC trace of the polymeric compound containing quinoline showed no crystallization but only melting and glass transitions peaks. This clearly indicates that the incorporation of the rigid quinoline unit into the phenyl backbone reduces the segmental mobility and effectively suppresses the tendency of the polymer chains to densely pack. This improved thermal resistance of the copolymers bodes well for stable blue emission from LEDs made from them

The DSC second heating scans of the polymeric compound are as shown in Fig. 10. Fig. 10 indicate that CL-OMe-DPQ undergoes a glass transition at 43 °C, following by melting point at 103 °C and degradation temperature at 303 °C. In contrast, there was no phase transition signal observed for [(CL-OMe-DPQ)₂ Ir(acac)] from 30 to 350 °C.

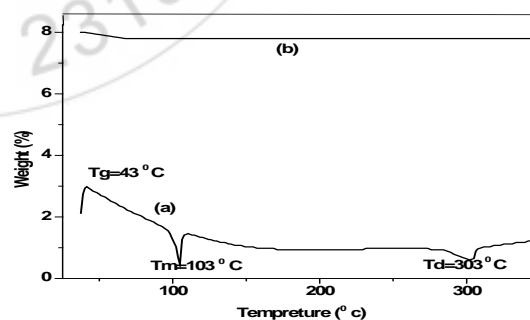


Figure 10: DSC scans of (a) CL-OMe – DPQ and (b) [(CL-OMe-DPQ)₂ Ir(acac)]

3.3 Optical Properties

3.3.1 Absorption Spectra: The absorbance and PL spectra of OMe - DPQ in different organic base solvents such as chloroform, dichloromethane and THF measured at room temperature are shown in fig 11. In figure 11 (curve a,b,&c), shows absorption spectra of OMe-DPQ in chloroform, dichloromethane and THF. The absorbance spectrum of the

compound is characterized by a strong absorption peak centered at 270 nm with a weak shoulder at 330 nm. This peak should be due to the diphenyl ring in OMe – DPQ.

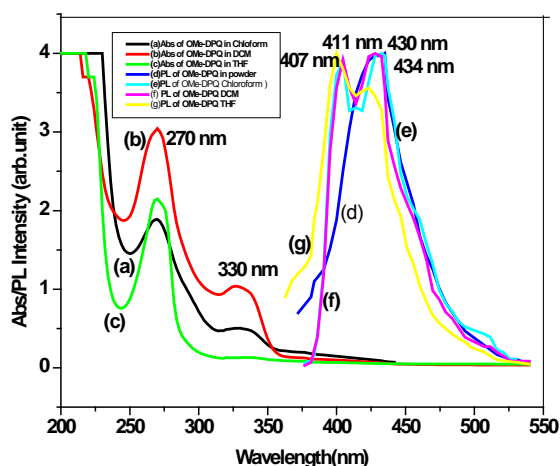


Figure 11: Absorption and PL spectra of OMe-DPQ in (a) Chloroform, (b) dichloromethane DCM & (c) THF Solution

The spectra are identical to that of 2, 4- DPQ as a result of the weak inductive effect of the methoxy group. The maximum peak observed for asymmetric OMe-DPQ exhibits a significant red shift relative to that of 2, 4- DPQ ($\lambda_{max} = 254$ nm), suggesting strong $\pi - \pi^*$ conjugation. This observation is consistent with a recent study on the distinct photophysical properties observed in 2, 4- DPQ. When compared the optical absorption of OMe-DPQ is bathochromically shifted by 10-15 nm, indicating that the methoxy substituent plays a role in determining the gap between the highest occupied molecular orbital (HOMO) and the lowest unoccupied molecular orbital (LUMO). We obtain the energy gap E_g Using the procedure described by Morita et al. [24] for energy gap determination for OMe-DPQ in chloroform, dichloromethane and THF (Fig.12).

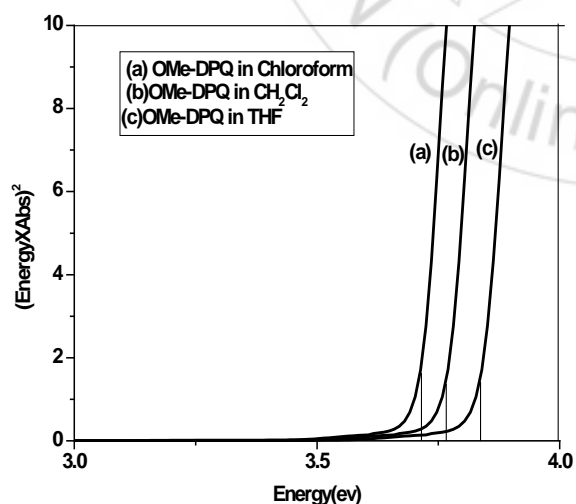


Figure 12: Determination of band gap E_g in (a) Chloroform, (b) DCM and (c) THF.

The optical band gaps (E_g) of the polymeric compound determined from the absorption edge were 3.695, 3.741 and 3.763 eV in Chloroform, DCM and THF respectively. The UV-vis absorption and PL spectra of OMe-DPQ in acid

solutions such as acetic acid and formic acid are as shown in Fig.13.

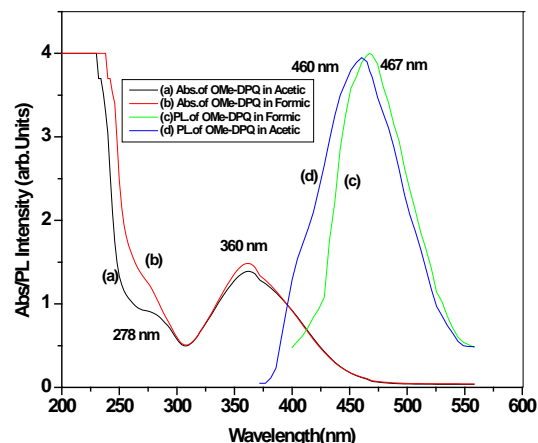


Figure 13: Absorption and PL spectra of OMe-DPQ in (a) Acetic acid and (b) Formic acid

The spectra of OMe-DPQ in acid solutions indicate that the electron donor substituents (methoxy) on the conjugated side chain of OMe-DPQ have little influence on the UV region absorption but have an obvious influence on the visible absorption of the polymeric compound solution. (The UV absorption peak of OMe-DPQ in acid is 21 nm red shifted in comparison with that of in CHCl_3 , CH_2Cl_2 and THF). The absorption peak is red-shifted, which indicates a lower $\pi - \pi^*$ transition energy or a lower band gap of the two polymers.

A strong absorption peak centered at 360 nm with a weak shoulder at 278 nm characterizes the absorbance spectrum of the compound. The peak at higher wavelength is attributed to $\pi - \pi^*$ interaction.

The absorption spectra of the polymeric compound OMe-DPQ in acetic acid and formic acid [Fig. 13 Curve (a), (b)] are dramatically different in line shape and absorption maxima compared to the spectra in aprotic organic solvents. The absorption maxima of OMe-DPQ in these solvents are 330 and 360 nm, respectively. Here, protonation of the quinoline moieties in the compound OMe-DPQ results in a much stronger electron-donating group, thereby enhancing charge separation of π - electrons in the conjugated donor-acceptor structure. The net effect of the protonation is thus an enhanced injected charge transfer (ICT) in acetic and formic acid compared to the aprotic organic solvents such as chloroform, Dichloromethane and THF.

Figure 13 Curve (c), & (d) PL spectra of the polymeric compound OMe-DPQ in formic and acetic acid with excitation wavelength 426 nm and 358 nm respectively at concentration 10^{-6} M. When the excitation wavelength was 426 nm, it was observed that the PL intensity is appeared at 467 nm. The excitation and PL spectra of the polymeric compound OMe-DPQ in acetic acid with excitation wavelength 358 nm at concentration 1×10^{-6} M are shown in figure 12 curves (d).

When the excitation wavelength was 358 nm, it was observed that the PL intensity peaks are appeared at 460 nm. The fluorescence spectrum of OMe-DPQ is slightly red

shifted (~35 nm) when compared to those of DPQ obtained under the same experimental conditions. The red shift of the PL spectra of OMe-DPQ with increasing solvent polarity is accompanied by significant broadening of the emission band, particularly in acetic acid. This shift could be due to a different rearrangement of solvent molecules in the transient ground state and singlet excited state, because of the presence of two flexible aliphatic chains in addition to an extra methoxy moiety.

The energy gap E_g Using the procedure described by Morita et al. for energy gap determination for OMe-DPQ in acetic acid and formic acid are as shown in Fig.14.

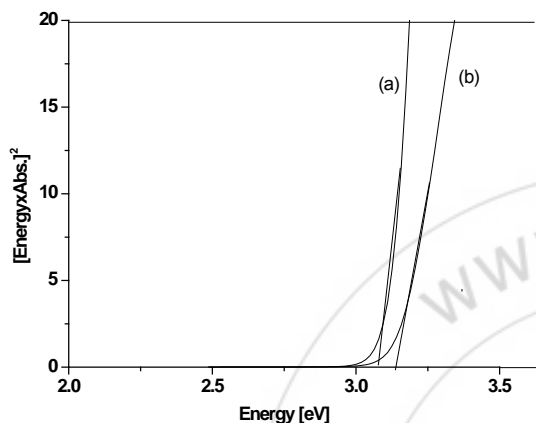


Figure 14: Determination of band gap E_g in (a) Acetic acid and (b) Formic acid

The optical band gaps (E_g) of the polymeric compound determined from the absorption edge were 3.078 and 3.143 eV in acetic acid and formic acid respectively.

We assign the strong absorption bands in the UV region to the spin-allowed $^1p-p^*$ transition of the cyclometalated quinoline ligands. The lowest energy absorption, with peak wavelengths in the region 440–460 nm, can be ascribed to a typical spin-allowed metal-to-ligand charge transfer (1MLCT) transition; we believe the weak bands at long wavelengths are associated with both spin-orbit coupling enhanced $3p-p^*$ and 3MLCT transitions. It is noteworthy that the formally spin forbidden 3MLCT gains intensity by mixing with the higher-lying 1MLCT transition through the strong spin-orbit coupling on Ir, which results in an intensity that is comparable with the allowed 1MLCT. We observed highly intense photoluminescence (PL) for (OMe-DPQ)₂ Ir (acac) in THF with values of λ_{max} located at 610 nm. (Fig.15) The broad, structure less spectral features lead us to conclude that the phosphorescence originates primarily from the 3MLCT state [21] (OMe-DPQ)₂ Ir (acac) shows absorption peak at 270, 330, 354, 427, 465, 510 nm in tetrahydrofuran solution. From this observation and by comparison with those of known complexes [19, 20], it is clear that the observed emission of the iridium complex is phosphorescent in nature. Further studies on its electro phosphorescence property are in progress.

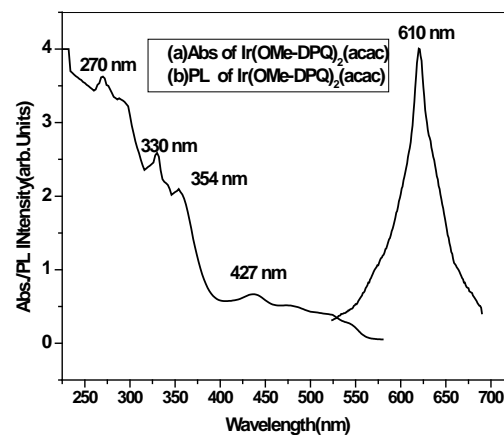


Figure 15: The UV-vis absorption and PL of Ir(OMe-DPQ)₂(acac)

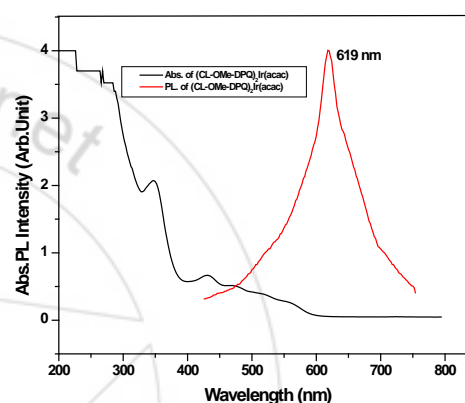


Figure 16: The UV-vis absorption and PL of Ir(CL-OMe-DPQ)₂(acac)

We observed highly intense photoluminescence (PL) for [(CL-OMe-DPQ)₂ Ir (acac)] in THF with values of λ_{max} located at 619 nm. (Fig.16) The broad, structure less spectral features lead us to conclude that the phosphorescence originates primarily from the 3MLCT state [21] (OMe-DPQ)₂ Ir (acac) shows absorption peak at 263, 335, 442, 479, 508 and 539 nm in dichloromethane solution. From this observation and by comparison with those of known complexes [19, 20], it is clear that the observed emission of the iridium complex is phosphorescent in nature. Further studies on its electro phosphorescence property are in progress.

4. Conclusion

We have successfully synthesized a new red emitting soluble Ir(III) phosphorescent complexes [(OMe-DPQ)₂ Ir (acac)], bearing a 2-(4-Methoxy-phenyl)-4-phenyl-quinoline (OMe-DPQ) ligand and [(CL-OMe-DPQ)₂ Ir (acac)], bearing a 4-chloro-2-(4-Methoxy-phenyl)-4-phenyl-quinoline (CL-OMe-DPQ) ligand. The synthesized complexes is thermally very stable over a wide range of temperature and suitable for the use as a red-emissive material in solution processed organic devices. In conclusion, the synthesized [(OMe-DPQ)₂ Ir (acac)], [(CL-OMe-DPQ)₂ Ir (acac)] complexes with the emission in the red region at 610 nm and 619 nm is very promising for applications in flexible organic devices.

References

- [1] C.H. Chien, C.K. Chen, F.M. Hsu, C.F. Shu, P.T. Chou, C.H. Lai, *Adv. Funct. Mater.* 19 (2009) 560–566.
- [2] X. Xing, L. Zhang, R. Liu, S. Li, B. Qu, Z. Chen, W. Sun, L. Xiao, Q. Gong, *ACS Appl. Mater. Interf.* 4 (2012) 2877–2880.
- [3] L. Xiao, Z. Chen, B. Qu, J. Luo, S. Kong, Q. Gong, J. Kido, *Adv. Mater.* 23 (2011) 926–952.
- [4] R. Ragni, E. Plummer, K. Brunner, J.W. Hofstraat, F. Babudri, G.M. Farinola, F. Naso, L. De Cola, *J. Mater. Chem.* 16 (2006) 1161–1170.
- [5] H.K. Dahule, S.J. Dhoble, J.-S. Ahn, Ramchandra P. J. of Phy and Che of Solids 72 (2011) 1524–.
- [6] H.K. Dahule, S.J. Dhoble *J of Chemical, Biological and Physical Sciences* 2&3 (2012), 1539-1550.
- [7] J. Park, J. S. Park, Y. G. Park, J. Y. Lee, J. W. Kang, J. Liu, L. Dai, S.-H. Jin, *Organic Electronics* 14 (2013) 2114–2123
- [8] S.B. Raut, S.J. Dhoble and R.G. Atram, *Synthetic Metals* 2011, 161, 391.
- [9] R.N. Bera, N. Cumpstey, P.L. Burn, I.D.W. Samuel, *Adv. Funct. Mater.* 17 (2007) 1149–1152.
- [10] P. Wellmann, M. Hofmann, O. Zeika, A. Werner, J. Birnstock, R. Meerheim, G.F. He, K. Walzer, M. Pfeiffer, K. Leo, *J. Soc. Inf. Display* 13 (2005) 393–397.
- [11] M. Cai, T. Xiao, E. Hellerich, Y. Chen, R.J. Shinar, *Adv. Mater.* 23 (2011) 3590–3596.
- [12] S. Ye, Y. Liu, K. Lu, W. Wu, C. Du, Y. Liu, H. Liu, T. Wu, G. Yu, *Adv. Funct. Mater.* 20 (2010) 3125–3135.
- [13] E. Ahmed, T. Earmme, S.A. Jenekhe, *Adv. Funct. Mater.* 21 (2011) 3889–3899.
- [14] Y. Yang, Y. Zhou, Q. He, C. Yang, F. Bai, Y. Li, J. Phys. Chem. B. 113 (2009) 7745–7752.
- [15] S. Feng, L. Duan, L. Hou, J. Qiao, D. Zhang, G. Dong, L. Wang, Y.A. Qiu, *J. Phys. Chem. C.* 115 (2011) 14278–14284.
- [16] J.-P. Duan; P.-P. Sun; C.-H. Cheng, *Adv. Mater.* **2003**, 15, 224
- [17] V.V. Grushin, N. Herron, D.D. LeCloux, W.J. Marshall, V.A. Petrov, Y. Wang, *Chem. Commun.* 2001, 1494;
- [18] S. Lamansky, P. Djurovich, D. Murphy, F. Abdel-Razzaq, H.E. Lee, C. Adachi, P.E. Burrows, S.R. Forrest, M.E. Thompson, *Am. Chem. Soc.* **2001**, 123, 4304;
- [19] M.A. Baldo, M.E. Thompson, S.R. Forrest, *Nature* **2000**, 403, 750
- [20] J.C. Ostrowski, M.R. Robinson, A.J. Heeger, G.C. Bazan, *Chem. Commun.* **2002**, 784.
- [21] X. Gong, J.C. Ostrowski, G.C. Bazan, D. Moses, A. Heeger, *J. Appl. Phys. Lett.* **2002**, 81, 3711.
- [22] Y.-J. Su, H.L. Lung, C.L. Li, C.H. Chien, Y.T. Tao, P.T. Chou, S. Datta, R.S. Liu, *Adv. Mater.* **2003**, 11, 884.
- [23] E.A. Fehnel, *J. Org. Chem.* 31 (**1966**) 2899.
- [24] L. Lu, S.A. Jenekhe, *Macromolecules* **2001**, 34, 6249.
- [25] J.M. Hancock, S.A. Jenekhe, *Macromolecules* **2008**, 41, 6864.
- [26] S. Morita, T. Akashi, A. Fujii, M. Yoshida, Y. Ohmori, K. Yoshimoto, T. Kawai, A.A. Zakhidrov, S.B. Lee, K. Yoshino, *Synth. Met.* **1995**, 69, 433.
- [27] A. Tsuboyama, H. Iwawaki, M. Furugori, T. Mukaide, J. Kamatani, S. Igawa, T. Moriyama, S. Miura, T. Takiguchi, S. Okada, M. Hoshino, K. Ueno, *J. Am. Chem. Soc.* **2003**, 125, 12971.
- [28] A. Ohta, S. Masano, S. Iwakura, H. Watahiki, M. Tsutsui, Y. Akita, T. Watanabe, *J. Heterocyc. Chem.* **1982**, 19, 465.